Sensors & Transducers, Vol. 179, Issue 9, September 2014, pp. 180-187

Sensors & Transducers

Feature Recognition of Froth Images Based on Energy Distribution Characteristics

[1, 2] WU Yanpeng, [1, 3] PENG Xiaoqi, [1] ZHANG Jianzhi, [1] JIANG Qian
[1] School of Energy Science and Engineering, Central South University,
Changsha, Hunan 410083, China
[2] Department of Information Engineering, Shaoyang University, Shaoyang, Hunan 422000, China
[3] Department of Information Science and Engineering, Hunan First Normal University,
Changsha, Hunan 410205, China
[1] Tel.: +86 13667209882
E-mail: 1357827972@qq.com

Received: 22 May 2014 /Accepted: 29 August 2014 /Published: 30 September 2014

Abstract: This paper proposes a determining algorithm for froth image features based on the amplitude spectrum energy statistics by applying Fast Fourier Transformation to analyze the energy distribution of various-sized froth. The proposed algorithm has been used to do a froth feature analysis of the froth images from the alumina flotation processing site, and the results show that the consistency rate reaches 98.1 % and the usability rate 94.2 %; with its good robustness and high efficiency, the algorithm is quite suitable for flotation processing state recognition. *Copyright © 2014 IFSA Publishing, S. L.*

Keywords: Flotation, Froth image, Fast Fourier transform, Energy spectrum, Energy distribution.

1. Introduction

Flotation is widely used in complex mineral beneficiation process. During flotation production, the operators usually control the production process by judging the flotation froth state, leading to the result that the flotation yield and product quality are heavily dependent on the operator's experience and work attitude [1]. With the development of modern information technology, the flotation process-control technology based on machine vision can reduce working intensity and improve production focalization, thus being paid more attention to [2].

The flotation froth contains a large quantity of information closely related to the flotation process variables and flotation results, such as froth size distribution [3], the RGB component distribution [4], as well as velocity [5], etc., wherein the froth size distribution is the most important feature to indicate production state. In the flotation site, operators judge the mineralization degree mainly on the basis of the froth size.

There are two main froth size distribution analysis methods. One is based on image segmentation method [6, 7]. Zhou Kaijun et al made a quantitative description of the froth shape and size features by splitting froth images, providing data support for the flotation process [8]; and Zeng Rong applied froth edge heuristics and watershed segmentation method to split the images [9]. Such methods enjoy a high recognition rate of image features, but its algorithm is complex with low real-time performance. Another method is to determine based on froth characteristics. Bartolacci used gray level co-occurrence matrix and wavelet analysis to extract froth pattern and the least squares method to establish empirical model of the

concentrate ore grades, thus realizing a feedback control over the flotation process [10]. Moolman obtained the average size of the copper ore flotation froth based on image color analysis and Fast Fourier Transform algorithm, but the method cannot be used to match the flotation conditions [11]. Liu proposed a novel image analysis solution based on multiresolutional multivariate image analysis (MR-MIA) for the monitoring and control of flotation processes. Marais established the nonlinear relationship between the image variables and process conditions and the froth flotation grades by using artificial neural networks (ANN) [12]. These feature determination algorithm is relatively simple, with good real-time performance; but the calculation is rough, with bigger error, and lacks determination of the essential froth characteristics [13]. Gui Weihua proposed froth texture extraction described by texture complexity based on color co-occurrence matrix [14]. In this paper, a Fast Fourier Transform analysis of the energy distribution of different-sized froth is made to identify the correspondence between the froth size and energy distribution, and a froth image feature analysis algorithm is proposed on the basis of Fast Fourier Transform to realize a fast determination of the flotation froth conditions.

2. Flotation Froth Image Characteristics

2.1. Definition of the Basic Characteristics of the Flotation Froth Image

At the flotation industrial site, the operators judge the flotation conditions according to the size and number distribution of froth [15]. The froth is traditionally divided into three categories: large, medium and small. It is generally thought a large froth has a poor degree of mineralization and carries a small number of concentrate ore; a medium froth has a good mineralization degree, while a small one has high degree of mineralization but low recovery rate. In order to accurately define the flotation conditions, we need to define the six basic characteristics of the froth image, as shown in Table 1.

Table 1. Characteristics of the flotation froth image.

Image class	Characteristics definition	Symbol	Description
Large	A large number of large froth	A	Large image occupies more than 50 % area.
	A fairly large number of large froth	a	Large image occupies more than 20 % area.
Medium	A large number of medium froth	B	Medium image occupies more than 50 % area.
	A fairly large number of medium froth	b	Medium image occupies more than 20 % area.
Small	A large number of small froth	C	Small image occupies more than 50 % area.
	A fairly large number of small froth	c	Small image occupies more than 20 % area.

According to the froth image definition, froth image may be of a single feature, such as "A", "B", "C", etc., and can also be a combination of features, such as "Ab", "abc", "Bc", "bC", etc.

2.2. Flotation Froth Image Acquisition

The flotation process is usually carried out in a confined environment. To acquire a real-time access to the flotation froth image, we placed just above the flotation tank a high-speed digital video camera and light source, and the photographs taken at fixed times would be transmitted over the network to a computer for data processing. Fig. 1 shows a typical alumina flotation froth image. In fact, the shooting environment of most flotation processing sites is so bad that the quality of the obtained froth images not very high.

Quality of foam images is generally considered influenced by following factors:

(A) Light intensity: the impact of the average luminance value of the bubble image.

(B) Position of the light source: the impact of the location and size of the bright area at the top of the foam.

(C) Light reflectance of foam surface: inversely proportional to the roughness of foam surface.

(D) Camera exposure: white color strengthened (plus exposure) or decreased (less exposure).

(E) Camera Sensitivity: rate of light acceptance.

(F) Camera shutter speed: may cause ghosting, smear phenomenon.

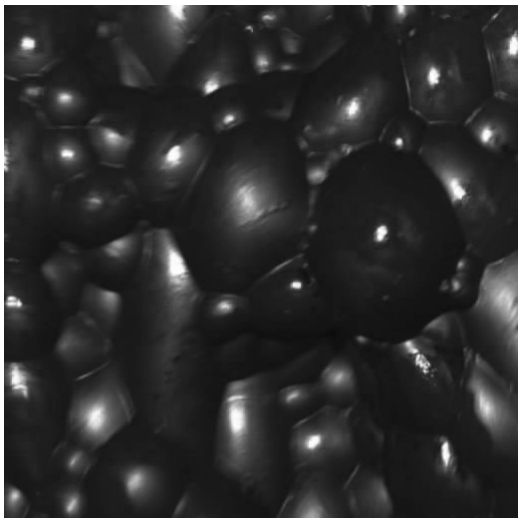

Fig. 1. Typical froth image.

The froth image quality influencing factor (F) is the most important reason to justify the unreliability.

With specified light intensity and light source position, same degree of camera exposure and sensitivity, and ignoring influence factors of the light reflectance of the foam surface, the distribution range of bubble size and bubble count of foam image can be determined by statistical methods, and then to determine foam image features.

Unfortunately, however, above conditions are difficult to meet.

Assume that all the bubbles in the froth image are floating at the top of the mother liquor, basically tile-like with fewer layers. According to the spectral theory, there are more low-frequency components in large froth's image spectrum, while there are more high-frequency components in the small forth's image spectrum. That is to say, the more large froth in the image, the more long-amplitude components in the amplitude spectrum; and the more small froth, the less long-amplitude components. Theoretically, the statistical analysis of different lengths of amplitudes in the amplitude spectrum of the froth image such as the number, the average value, and so on, can help judge the size and number distribution features of the froth image.

The flotation process is usually carried out in a confined environment. To obtain real-time flotation froth images, we placed a high-speed digital video camera and a light source above the flotation tank, photographed and transmitted over network to a computer for processing. In fact, most shooting environment of the flotation process is so bad that the quality of obtained image is usually poor.

2.3. Basic Ideas of Determining the Froth Image Features Based on the Amplitude Spectrum's Energy Statistics

In order to solve the difficulties caused by low quality images to the froth image feature analysis, we proposed a method to determine the flotation froth image features based on the amplitude spectrum's energy statistics, and the basic ideas and steps are as follow:

Image Gray Value Normalization. Froth image is pre-processed to calculate the mean value of the average luminance value of the froth image, remove images with too much deviation of the luminance value, and all the remaining froth images' average luminance value is changed to the mean value of the average luminance value one by one. Thus, you can basically eliminate the influence of factors (A), (C), (D), and (E) on froth image quality.

Froth Image Characteristic Value. The amplitude length in the amplitude spectrum is classified, and the ability of each amplitude class is summed to get the froth image feature value. Compared with the value range of the statistical results, the value range of energy summation is greater than that of numeral summation and help to conduct feature classification; at the same time, it can eliminate the influence of factor (B) on the froth image characteristics.

The Formula to Determine the Froth Image Features and Its Threshold. The statistical analysis of the correspondence between the froth image features and froth image feature values determines the valid value range of a variety of froth image features corresponding to the froth image feature value, and then confirms the formula to judge froth image features as well as its parameters.

Froth Image Characteristic Determination and Its Effectiveness Analysis. The froth image feature-determining formula is used to ascertain the froth image characteristics, and the results will undergo a validity analysis. According to the formula, the feature of the forth image x is y, but the x's feature value in not within the valid value range of the froth image feature y, so it's obvious that the froth image feature determination results are not reliable.

3. The Flotation Froth Image Feature Determining Algorithm based on the Amplitude Spectrum's Energy Statistics

The use of Fast Fourier Transform to generate the Fourier spectrum is a commonly used method for frequency domain analysis, and widely used in such fields as digital image processing [16].

3.1. Fast Fourier Transform

Let the image data be $f(x, y)$ (x = 0, 1... M-1; y = 0, 1, N-1), then the discrete Fourier transform is:

$$F(u,v) = \frac{1}{MN}\sum_{x=0}^{M-1}\sum_{y=0}^{N-1} f(x,y)e^{-i2\pi\left(\frac{ux}{M}+\frac{vy}{N}\right)}, \quad (1)$$

Where u = 0, 1... M-1; v = 0, 1, N-1.

The inverse transformation formula of formula (1) is:

$$f(x,y) = \frac{1}{MN}\sum_{u=0}^{M-1}\sum_{v=0}^{N-1} F(u,v)e^{i2\pi\left(\frac{ux}{M}+\frac{vy}{N}\right)}, \quad (2)$$

where x=0, 1, M-1; y= 0, 1, N-1.

When M = N, the discrete Fourier transform is:

$$\begin{aligned} F(u,v) &= \frac{1}{NN}\sum_{x=0}^{N-1}\sum_{y=0}^{N-1} f(x,y)e^{-i2\pi\frac{ux+vy}{N}} \\ &= \frac{1}{N}\sum_{x=0}^{N-1}(x,y)e^{-i2\pi\frac{ux}{N}}\cdot\frac{1}{N}\sum_{y=0}^{N-1} f(x,y)e^{-i2\pi\frac{vy}{N}}, \end{aligned} \quad (3)$$

where u = 0, 1... M-1; v = 0, 1, N-1.

The inverse transformation formula of formula (3) is:

$$f(x,y) = \frac{1}{NN}\sum_{u=0}^{N-1}\sum_{v=0}^{N-1} F(u,v)e^{i2\pi\frac{ux+vy}{N}} = \frac{1}{N}\sum_{u=0}^{N-1} F(u,v)e^{i2\pi\frac{ux}{N}} \cdot \frac{1}{N}\sum_{v=0}^{N-1} F(u,v)e^{i2\pi\frac{vy}{N}}, \quad (4)$$

To calculate the two-dimensional Fast Fourier Transform of $f(x, y)$, we first calculate the one-dimensional Fourier transform along each column and then along each of its rows, i.e.:

3.2. The Fast Fourier Transform of the Froth Image

The Fourier spectrum of the image $f(x, y)$ consists of amplitude spectrum and phase spectrum, wherein the amplitude spectrum is:

$$|F(u,v)| = \sqrt{R^2(u,v) + I^2(u,v)}, \quad (5)$$

The phase spectrum:

$$\varphi(u,v) = arctg\frac{I(u,v)}{R(u,v)}, \quad (6)$$

The energy spectrum of the image $f(x, y)$, is:

$$E(u,v) = |F(u,v)|^2 = R^2(u,v) + I^2(u,v), \quad (7)$$

The froth image is composed of froth of different sizes and the background [17]. Considering the sharpness of the image and the factor of operation speed, we chose the middle of the froth image, i.e., area n × n (n=22 k), and applied the Fast Fourier Transform processing to obtain the spectrum image as shown in Fig. 2 [18]. Frequency spectrum of froth image with DC component shifted to center is shown in Fig. 3.

Fig. 4 and Fig. 5 show typical spectrum energy count and sum distribution of froth images.

3.3. Statistics of Spectrum Energy

According to spectral theory, in the low energy statistical region, the small froth has the highest energy, the medium froth less high, and the large froth the lowest respectively, while in the high energy statistical region, the large froth has the highest energy, the medium froth less high, and the small froth the lowest respectively.

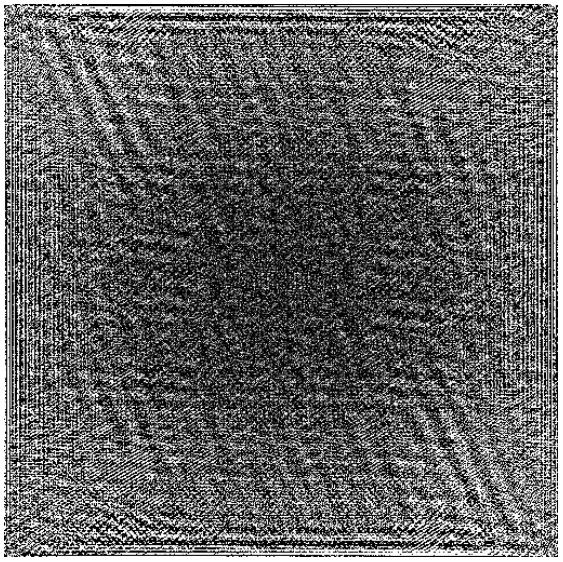

Fig. 2. Frequency spectrum of froth image.

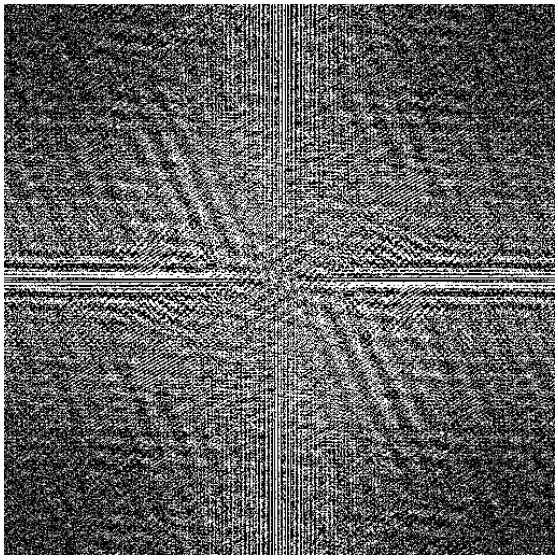

Fig. 3. Frequency spectrum of froth image with DC component shifted to center.

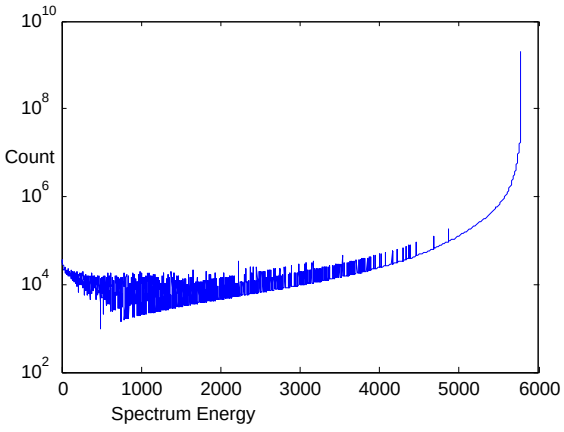

Fig. 4. Spectrum energy count distribution of froth image.

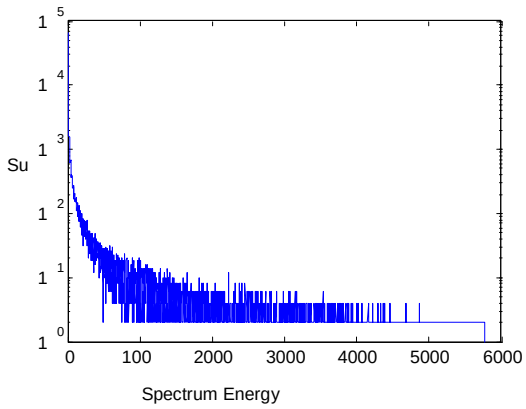

Fig. 5. Spectrum energy sum distribution of froth image.

We calculated the gray scale normalization, and the linearity of the average gray scale of all froth images was adjusted to 0.20. Fig. 6, Fig. 8, Fig. 10 shows froth images with different size bubbles, and Fig. 7, Fig. 9, Fig. 11, respectively, shows their spectrum energy statistical result.

It can be easily seen that the froth image with small bubbles gets a declining energy statistical curve, while the froth image with large bubbles gets a flat energy statistical curve.

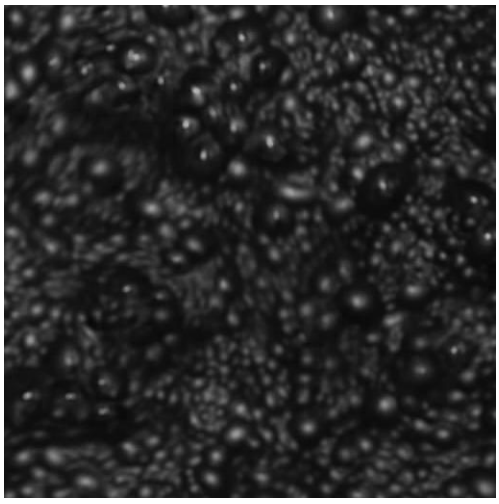

Fig. 6. Froth image with small bubbles.

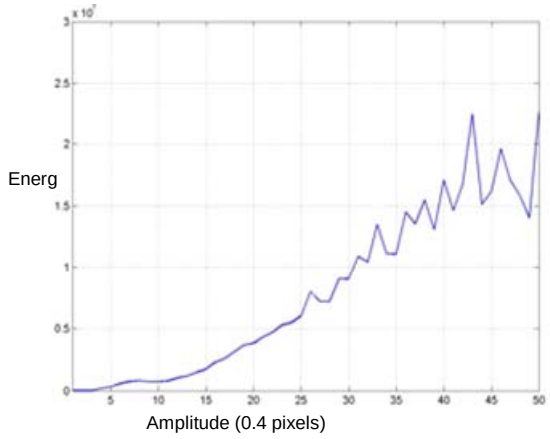

Fig. 7. Spectrum energy statistics of froth image with small bubbles.

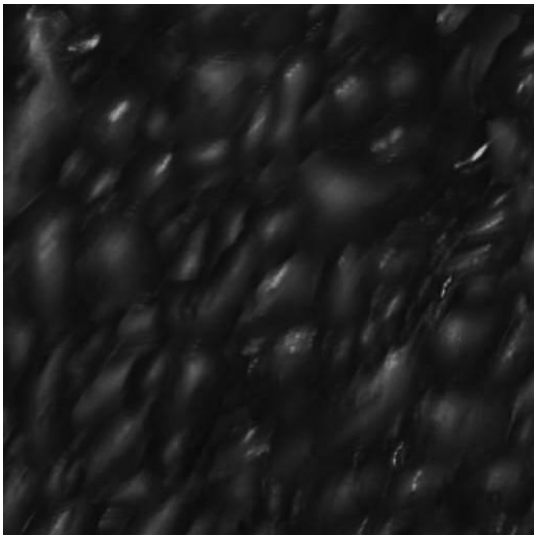

Fig. 8. Froth image with middle bubbles.

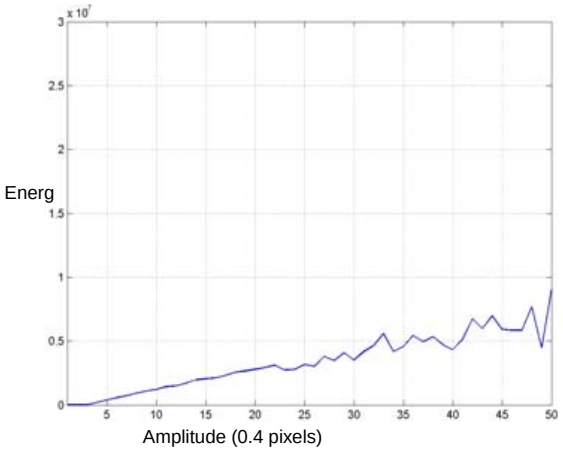

Fig. 9. Spectrum energy statistics of froth image with small bubbles.

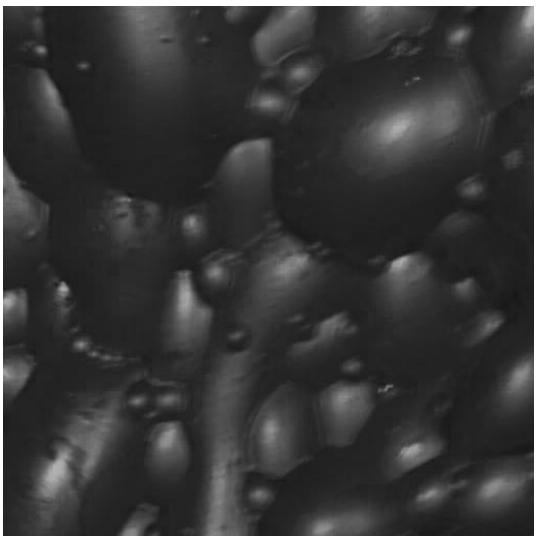

Fig. 10. Froth image with large bubbles.

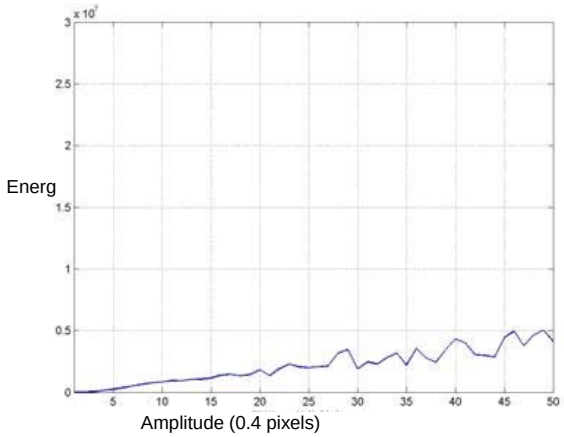

Fig. 11. Spectrum energy statistics of froth image with large bubbles.

3.4. Feature-determining Formula of the Froth Image

Let e_0 be the sum of energy of region (0,529], e_1 be the sum of energy of region (530, 1225], e_2 be the sum of energy of region (1226, 2916], and e_3 be the sum of energy of region (2917, 6241].

Also define symbols as following:

$$x_1 = \frac{e_1}{e_2+e_3}, \tag{8}$$

$$x_2 = \frac{e_2}{e_1+e_3}, \tag{9}$$

$$x_3 = \frac{e_3}{e_1+e_2}, \tag{10}$$

Then we can get feature-determining formula for each class of froth image.

$$t = \begin{cases} A, if\ x_3 \geq p_A \\ a, if\ p_A > x_3 \geq p_a \\ B, if\ (x_3 < p_A) \cap (x_1 < p_a) \cap (x_2 \geq p_B) \\ b, if\ ((x_3 \geq p_A) \cup (x_1 < p_a) \cap (x_2 \geq p_{AB})) \cup \\ \quad ((x_3 < p_A) \cap (x_1 < p_a) \cap (x_2 < p_B) \cap (x_2 > p_b)) \\ C, if\ x_1 \geq p_C \\ c, if\ p_C > x_1 \geq p_c \end{cases}, \tag{11}$$

where P_A, P_a, P_B, P_b, P_{AB}, P_C, P_c are the underdetermined parameters.

4. Simulations and Result Analysis

4.1. Simulation Environment

52 clear froth images shot in the same amount of light at the alumina flotation industrial field were chosen, and the central rectangular area (512 × 512) of each image is used to determine the froth features. Then an experimental platform was established in a Lenovo computer whose CPU is Intel i3 3.2 GHz, with a 2.99 GB memory. According to the method presented in this paper, the Matlab simulation program was compiled to do simulation calculation of the chosen froth images in the debug mode.

4.2. Parameter Assignment

We made a statistical analysis of the energy distribution of the 16 froth images, and then proposed the froth image feature-determining formula and their definitions, coupled with the determining formula's parameters. Result of froth image features determining is shown in Table 2.

Table 2. Froth image features determining.

Image ordinal	Artificial determination	e_1	e_2	e_3	x_1	x_2	x_3	Program-based determination
1	Ab	101946640	222565521	55468555	0.17	1.413	0.366	Ab
2	Ab	76354709	157970886	79658529	0.339	1.012	0.321	Ab
3	aB	226886884	478817239	22325114	0.031	1.921	0.452	aB
4	Ab	87826670	221589134	82125534	0.265	1.303	0.289	Ab
5	Ab	105991581	198973705	122629049	0.402	0.87	0.329	Ab
6	Ab	258060480	513472839	125887010	0.163	1.337	0.403	Ab
7	Ab	102234611	252580677	174868921	0.492	0.911	0.239	Ab
8	Ab	248726668	446402457	116381314	0.167	1.222	0.441	Ab
9	aB	260033930	441616167	89069993	0.126	1.264	0.489	aB
10	Ab	271400789	459248925	119043944	0.162	1.176	0.469	Ab
11	aB	250572900	482271926	76466651	0.104	1.474	0.448	aB
12	aB	268689106	507020918	66416170	0.085	1.513	0.468	aB
13	aB	251331702	439791716	23054864	0.033	1.602	0.543	aB
14	aB	312200323	392913564	81084087	0.114	0.999	0.658	aB
15	Ab	270775588	443734647	129139174	0.18	1.109	0.472	Ab
16	aB	253246649	493500097	74318181	0.099	1.506	0.445	aB

Parameters of formula (11) are assigned as shown in Table 3.

Table 3. Parameters Assignment.

P_A,	P_a	P_B	P_b	P_{AB}	P_C	P_c
0.15	0.01	0.4	0.1	0.09	3.0	1.68

4.3. Froth Image Features Determining

The large froth images with an energy total lower than 3*10^8 as well as the medium and small froth images with an energy total lower than 2*10^8 are defined as unqualified images.

The features of all rest froth images are ascertained according to the determining formula are shown in Table 4.

Table 4. Result of rest froth image features determining.

Artificial determination	x_1	x_2	x_3	Program-based determination
abc	0.098	1.145	0.603	aB
abc	0	0.398	2.51	*
B	0	0.887	1.126	B
Bc	0	0.44	2.269	Bc
Bc	0	0.555	1.801	Bc
Bc	0	0.555	1.801	Bc
bC	0	0.23	4.337	bC
bC	0	0.149	6.68	bC
bC	0.081	0.116	4.568	bC
bC	0	0.197	5.063	bC
Ab	0.165	0.978	0.571	Ab
Ab	0.203	1.373	0.337	Ab
aB	0.042	1.786	0.467	aB
Ab	0.41	0.776	0.373	Ab
Ab	0.222	1.013	0.458	Ab
Ab	0.42	0.973	0.266	Ab
Ab	0.354	1.049	0.292	Ab
aB	0.067	1.709	0.439	aB
aB	0.081	1.802	0.391	aB
aB	0.125	1.208	0.518	aB
aB	0.066	1.379	0.557	aB
Ab	0.42	0.973	0.266	Ab
aB	0.019	1.7	0.541	aB
aB	0.113	1.201	0.544	aB
aB	0.052	0.91	0.901	aB
B	0	1.093	0.914	B
Ab	0.178	1.012	0.527	Ab
abc	0	0.683	1.463	*
B	0	0.597	1.672	B
Bc	0	0.594	1.682	Bc
Bc	0	0.537	1.861	Bc
Bc	0	0.407	2.456	Bc
abc	0	0		*
bC	0	0.258	3.872	bC
bC	0	0.139	7.145	bC
bC	0	0.292	3.419	bC

Note: Images fail to determinate are marked as "*".

4.4. The Calculation Results Analysis

The calculation results show that:

The results of the program-based determination of the froth image map features match the results of the artificial determination at the rate of 98.1 %, meaning that the proposed algorithm is quite accurate, and is able to reflect the exact characteristics of the froth image. The accuracy of froth image features determination is shown in Fig.12.

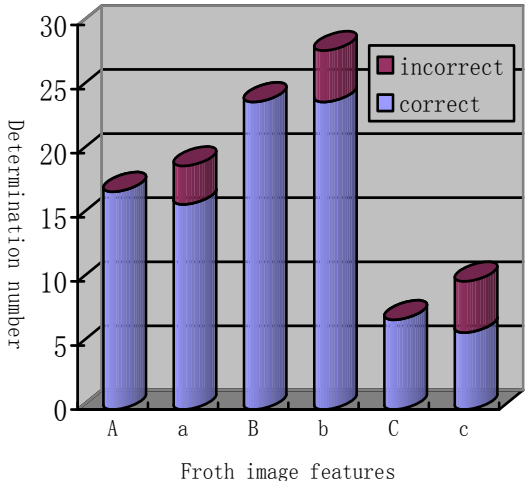

Fig. 12. Accuracy of froth image features determination.

94.2 % images are qualified, meaning that the proposed algorithm is highly adaptive. The reason why 3 images are marked as "*" is because the algorithm cannot identify whether they are "abc" style images or faulty images.

The average processing time for each frame of image is 0.3 s, indicating that the proposed method is highly efficient with a good real-time performance, thus being practically suitable for real-time industrial control.

5. Conclusions

According to the spectrum theory, there is an intrinsic link between the flotation froth image size and image energy. This paper analyzes the energy distribution characteristics of the froth map, proposes a decision algorithm of froth image features based on the amplitude spectrum energy statistics. Aluminum oxide froth image experiment and analysis results show that the proposed algorithm is accurate, highly efficient, with good real-time performance.

The froth image analysis results were affected by a variety of factors such as the photo light intensity, the position of the light source, froth flow speed, the camera shutter speed and so on. The next step will be to do quantitative analysis of froth image spectroscopy influenced by the factors discussed above, and to research the application of the BP neural network which is capable of self-learning.

Acknowledgements

This work is supported by Natural Science Foundation of China (No. 61134006), Natural Science Foundation of China (No. 61273169), Hunan Province Science Foundation of China (No. 14JJ7077) and Fund of Hunan Provincial Education Department of China (13B107).

References

[1]. V. I. Melik-Gaikazyan, and N. P. Emel'yanova, Competitive representations in studies on froth flotation and prospects of their application for selection of reagents, *Russian Journal of Non-Ferrous Metals*, Vol. 48, 2007, pp. 237-251.

[2]. Wang Jian-Kun, Research on identification of characteristics for froth image in flotation process, *Yunnan Metallurgy*, Vol. 1, 2009, pp. 65-67.

[3]. He Guichun, Huang Kaiqi, Study of the relation between flotation indexes and froth digital images, *Metal Mine*, Vol. 8, 2008, pp. 97-101.

[4]. J. Hatonen, H. Hyotylliemi, J. Miettunen, Using image information and partial least squares method to estimate mineral concentrations in mineral flotation, in *Proceedings of the Second International Conference on Intelligent Processing and Manufacturing of Materials*, Hawaii, USA, 1999, pp. 459-464.

[5]. Mu Xuemin, Liu Jinping, Gui Weihua, et al, Flotation froth motion velocity extraction and analysis based on SIFT features registration, *Information and Control*, Vol. 4, 20116 pp. 525-531.

[6]. John A. Bogovic, Jerry L. Prince, and Pierre-Louis Bazin, A multiple object geometric deformable model for image segmentation, *Computer Vision and Image Understanding*, Vol. 117, 2013, pp. 145-157.

[7]. Guoying Zhang, Zhu Hong, and Xu Ning, Flotation bubble image segmentation based on seed region boundary growing, *Mining Science and Technology*, Vol. 21, pp. 239-242, 2011.

[8]. Zhou Kai-Jun, Wang Yi-Jun, Xu Can-Hui, Froth morphological feature extraction based on improved FCM and mathematic morphology segmentation. *Journal of Central South University (Science and Technology)*, Vol. 43, 2010, pp. 994-1000.

[9]. Zeng Rong, Study of edge detection methods on flotation froth image, *Journal of China University of Mining & Technology*, Vol. 31, 2002, pp. 421-425.

[10]. G. Bartolacci, P. Pelletier, J. Tessier, et al, Application of numerical image analysis to process diagnosis and physical parameter measurement in mineral processes-part 1 flotation control based on froth textural characteristics, *Minerals Engineering*, Vol. 6, 2006, pp. 734-747.

[11]. D. W. Moolman, C. Aldrich, J. S. J. Van Deventer, et al, Digital image processing as a tool for on-line monitoring of froth in flotation plants, *Minerals Engineering*, Vol. 9, 1994, pp. 1149-1164.

[12]. J. J. Liu, et al, Flotation froth monitoring using multiresolutional multivariate image analysis, *Minerals Engineering*, Vol. 18, 2005, pp. 65-76.

[13]. C. Marais and C. Aldrich, The estimation of platinum flotation grade from froth image features by using artificial neural networks, *Journal of the South African Institute of Mining and Metallurgy*, Vol. 111, 2011, pp. 81-85.

[14]. Gui Weihua, et al, Color co-occurrence matrix based froth image texture extraction for mineral flotation, *Minerals Engineering*, Vol. 46, 2013, pp. 60-67.

[15]. P. Patra, et al, Transport of fibrous gangue mineral networks to froth by bubbles in flotation separation, *International Journal of Mineral Processing*, Vol. 104, 2012, pp. 45-48.

[16]. Georgios Tzimiropoulos, et al, Robust FFT-based scale-invariant image registration with image gradients, *Pattern Analysis and Machine Intelligence*, Vol. 32, 2010, pp. 1899-1906.

[17]. Gui Weihua, et al, Color co-occurrence matrix based froth image texture extraction for mineral flotation, *Minerals Engineering*, Vol. 46, 2013, pp. 60-67.

[18]. A. Averbuch, Y. Keller, FFT based image registration, in *Proceedings of the IEEE International Conference on Acoustics, Speech, and Signal Processing*, 2002, Vol. 4, pp. 3608-3611.